Growth factor delivery from hydrogel particle aggregates to promote tubular regeneration after acute kidney injury

Growth factor delivery from hydrogel particle aggregates to promote tubular regeneration after acute kidney injury

Journal of Controlled Release

Volume 167, Issue 3, 10 May 2013, Pages 248–255

Growth factor delivery from hydrogel particle aggregates to promote tubular regeneration after acute kidney injury

Mikhail V. Tsurkan;Peter V. Hauser;Andrea Zieris;Raquel Carvalhosa;Benedetta Bussolati;Uwe Freudenberg;Giovanni Camussi;Carsten Werner

Abstract

Local delivery of growth factors (GFs) can accelerate regeneration of injured tissue, but for many medical applications, injectable GF delivery systems are required for clinical success. Viscoelastic, injectable aggregates of micrometer-sized hydrogel particles made of multiarmed polyethylene glycol (starPEG) and heparin were prepared and tested for site-specific paracrine stimulation of tissue regeneration. Heparin was used as it binds, protects and releases numerous GFs. Hydrogel based delivery of basic fibroblast growth factor (bFGF) and murine epidermal growth factor (EGF) was monitored utilizing enzyme-linked immunosorbent assay (ELISA). bFGF was released slowly because of its high affinity to the heparin while the significantly higher release of the non-specific binding EGF was controlled by diffusion only. To investigate GF delivery *in vivo*, a hydrogel loaded with murine EGF or bFGF was injected subcapsularly into the left kidney of mice with experimental acute kidney injury caused by glycerol induced rhabdomyolysis. Visual examination confirmed sustained stability of the injected gel aggregates during the timescale of the experiment. The number of proliferating kidney tubular epithelial cells was quantified both in the injected kidney and the non-injected contralateral kidney. bFGF delivery from hydrogels induced a significant increase in cell proliferation in the injected kidney, although small effects were also seen in the non-injected kidney due to a systemic effect. EGF delivery strongly increased cell proliferation for both kidneys, but also showed a local effect on the injected kidney. The hydrogel without loaded GFs was used as a control and showed no increase in cell proliferation. Our results suggest that this novel starPEG-heparin hydrogel system can be an effective approach to deliver GFs locally.

1. Introduction

Regenerative medicine strives to develop therapies that restore normal function by repairing damaged organs and tissues or re-growing entire organs *de novo*. Organ repair can be performed *ex vivo*, for example by injection of embryonic or adult stem cells, or *in situ*, for example by delivering factors that will promote or enhance the repair mechanisms of the organ itself [1]. Within the last decade, many attempts have been made towards the development of a method for effective GF delivery *in vivo* to initiate cellular repair and tissue regeneration. Most of the attempts still show severe limitations, including a strong systemic effect of GFs which prevents the injection or oral delivery. One approach to overcome this limitation is to use a carrier material to store and release the GFs [2] and [3]. Among the variety of natural and artificial polymers that could be used as a GF carrier, heparin, a natural glycosaminoglycan, is attracting growing interest. Heparin is commonly used as an anticoagulant drug and is utilized for anticoagulant coatings [4]. Heparin's ability to bind and release a wide range of GFs has long been described [5] and efforts have been made to implement it as a component of biomaterials for cell culture and for GF delivery. Previous research has mostly focused on the chemical–physical properties and *in vitro* applications of heparin containing materials [6], [7], [8], [9], [10] and [11], while only a few reports describe their *in vivo* application [12], [13] and [14].

Recently, we presented a new biohybrid hydrogel platform that benefits from a great range of mechanical properties. The modular hydrogel is based on crosslinking multi-armed and end-functionalized (poly)ethyleneglycol (starPEG) with heparin. It combines the structural flexibility, hydrophilic character and repellent characteristics of star-shaped PEG, with the highly sulfated polysaccharide heparin, that has high affinity to various GFs. The gel has shown good biological potential in *in vitro* experiments by supporting a variety of cell types through GF delivery [15] and [16]. We further demonstrated the hydrogel's ability to release GFs in a controlled manner [17] and [18]. Further development of this hydrogel material is aimed towards its application as an injectable hydrogel. The implementation of injectable properties into a solid state material, such as a covalently cross-linked starPEG-heparin hydrogel, presents a problem to the gel's integrity. The gel needs viscous properties to be injectable, but should retain its elastic properties to hold its position in the dynamic environment of living tissue.

Acute kidney injury (AKI) is an immediate and extended reduction of the renal filtration rate. AKI has a high incidence rate worldwide and is one of the main complications during treatment in intensive care units [19] and [20]. Characteristics of AKI are epithelial injury due to tubular apoptosis and necrosis, tubular obstruction, vasoconstriction, changes of the filtration barrier and misfiltration [21] and [22]. Injection of mesenchymal stem cells (MSCs) into mice with experimental AKI can stimulate tubular regeneration and normalize renal function [23] and [24]. However, the injected stem cells localize infrequently to the site of tissue injury and therefore regenerative repair cannot be explained by trans-differentiated stem cells. It is hypothesized that tubules, which consist of tubular epithelial cells, are regenerated mostly by endocrine or paracrine stimulation [25] or by microvesicles produced from injected stem cells [26]. As the regenerative effects of these studies seem to be mainly attributed to secreted factors, we used the experimental AKI as a model to probe *in situ* regeneration by GFs [27].

The aim of this project was to develop an injectable hydrogel with viscoelastic properties that would serve as a local deposit for GFs to promote tubular proliferation in experimental AKI (Fig. 1). The viscous behavior of the material should allow its injection under the kidney capsule and the elastic properties should prevent erosion of the material out of the injected area. The hydrogel was loaded with bFGF or EGF, which have both been described to support regeneration after AKI [28], [29], [30] and [31], while injection of “empty” hydrogel was used as a control. bFGF has strong heparin affinity and is thought to be released slowly from the hydrogel [17] and [18]. It has been suggested that bFGF promotes renal repair *via* autocrine stimulation of the cells [32].

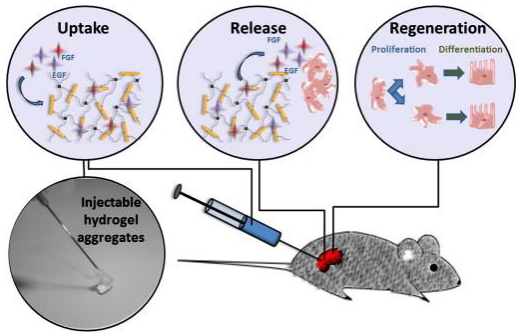

Fig. 1. .

Postulated treatment effect. The injectable hydrogel is loaded with non-covalently bound GFs. The viscoelastic properties of the hydrogel material allow its injection under the kidney capsule of a mouse with experimental AKI, but prevent erosion of the material from the injected area. The hydrogel serves as a local deposit for GFs in the injected area which is expected to stimulate epithelial cell proliferation and support regenerative repair.

There are numerous growth factors which do not have specific affinity to heparin, but still possess positively charged amino acid residues on their surfaces. Among them, murine EGF is well characterized and it has four arginine residues in the C-terminus, which can potentially serve in non-specific electrostatic attachment to heparin [33]. EGF has been described to enhance regenerative repair after kidney injury [34]. It was hypothesized that the high heparin content of the gel would slow down the release of EGF through non-specific electrostatic interactions. The aim was to evaluate the benefits of local EGF delivery in comparison to previously described subcutaneous GF administration [34].

2. Materials and methods

2.1. Chemicals

For the list of all chemicals see the Supplemental material.

2.2. Preparation of starPEG-heparin gels

Gels used for *in vivo* applications were prepared under sterile conditions and reagent solutions used in the preparation were sterilized by filtration through 0.2 μm PVDF filters (Life Science, Port Washington, USA). The gels were prepared as previously described [15]. Briefly, 2 × fold excess N-(3-dimethylaminopropyl)-N'-ethylcarbodiimide hydrochloride (EDC) and stoichiometric amount of *N*-hydroxysulfosuccinimide (NHS) were added to a pH 7 solution of heparin (MW 14,000) (Merck, Darmstadt, Germany) in phosphate buffered saline (PBS) (Sigma-Aldrich). To form a heparin-NHS ester, the reaction mixture was kept for 15 min at 4 °C. Next, a stoichiometric amount of four-armed polyethylene glycol (starPEG) (Mn = 10.0×10^3; PDI = 1.09) (Sigma-Aldrich) solution in PBS (pH 7.4) was added. The total volume of the reaction mixture was 1 ml and the total weight of heparin and starPEG mixture was about 110 mg (solid content 11%). The mixture gelated in less than 1 h, and was kept overnight at room temperature (RT) for the completion of the reaction. The gel was swollen in water and then in PBS to remove the side products of the reaction and stored in PBS at 4 °C.

2.3. Preparation of gel particles

Gel particles for *in vivo* applications were prepared under sterile conditions. To create gel particles, 1 ml of the gel was minced using a sterile spatula, collected with a 1 ml syringe and repeatedly pushed through a 0.9 mm needle (20G) until the gel was homogenized. The procedure was then repeated with a 0.45 mm needle (26G). Subsequently, the gel particles were washed with 1 ml MilliQ water (Millipore, Billerica, USA) by vortexing in a 2 ml vial until a transparent homogenous solution was generated. After centrifugation at 13.3 rpm for 2 min at RT, the solution separated into two fractions. The water containing upper fraction was removed by pipetting and the washing procedure was repeated twice with water and four times with PBS. The gel particles were stored in PBS at 4 °C.

2.4. Rheological measurements

Storage and loss moduli of the hydrogels were determined as previously described [15] and [16]. Briefly, oscillating measurements were performed on a rotational rheometer (Ares LN2, TA Instruments, Eschborn, Germany) with plate/plate arrangement (plate diameter 25 mm, gap width in the range of 1.1–0.8 mm). Frequency sweeps were carried out on materials swollen in PBS at RT in a shear frequency range of 10^{-1}–10^2 rad s^{-1} with the strain amplitude of 3%.

2.5. Laser scanning microscopy

Images of hydrogel particles were obtained using a confocal laser scanning microscope (TCS SP5 Leica, Bensheim, Germany) with a 10 × magnification objective (HCxPL APO CS 10 × 0.4 IMM, Leica) in DIC-mode (differential interference contrast). 1% Alexa488-labeled heparin was used for the preparation of the hydrogel imaged by fluorescence microscopy. The argon laser (excitation wavelength 488 nm, laser intensity 20%) was used for the imaging of Alexa-labeled gels. To measure the size of the particles, we used microscope software Leica LAS AF. The mean diameter of each particle was calculated as the sum of its largest and smallest dimensions divided by two.

2.6. Loading of the gel particles with bFGF and EGF

The PBS-swollen gel particles were centrifuged at 6.0 rpm for 1 min and the excess PBS was removed by decanting. Next, the gel was centrifuged at 13.3 rpm for 15 min and any remaining PBS was carefully removed with a syringe. The volume of the removed PBS was measured. The same volume of PBS containing 100 ng of dissolved EGF or bFGF (PeproTech GmbH, Hamburg, Germany) was added to the gel particles. The vial was extensively mixed by vortexing. The gel particles were swelled for 30 min and carefully collected by 1 ml syringes, approximately 100 μl per syringe. The syringes were hermetically closed and stored at 4 °C.

2.7. bFGF and EGF release experiment

Gel particles (50 μl, n = 5) were loaded with bFGF or EGF (1 μg/ml gel) as described in Section 2.6. Following immobilization, the particles were washed with 125 μl PBS/μl gel, while the washing solution was collected and stored at − 80 °C for analysis with ELISA (Quantikine kit, R&D Systems, Minneapolis, USA). GFs were then allowed to release from the particles at 37 °C into serum-free endothelial cell growth medium (ECGM; Promocell GmbH, Heidelberg, Germany) supplemented with 0.02% (v/v) Proclin 300 (Sigma-Aldrich) + 1 mg/ml bovine serum albumin (BSA, Sigma-Aldrich) (125 μl medium/μl gel). Following a short centrifugation step (5 min, 8000 rpm), samples were collected at 3, 18, 38 and 96 h and stored at − 80 °C until analysis by ELISA. An equal volume of fresh medium was added back at each time point.

2.8. Experimental AKI and hydrogel injection

Male C57B6 mice (Charles River, The Jackson Laboratory, Milano, Italy) were used at 8 to 10 weeks of age. Animals were housed under standardized conditions of 12 h light/12 h dark cycle, with no restrictions of food or water. Studies were conducted in accordance with the National Institutes of Health Guide for the Care and Use of Laboratory Animals. Glycerol induced rhabdomyolysis was induced in NN male C57B6 mice as described [35], [36] and [37]. In brief, mice (bodyweight ~ 30 g) were anesthetized and injected with 8 μl 50% glycerol per gram bodyweight into the left and right femoral muscle (Fig. 5A). Seventy-two hours following the administration of anesthesia, an incision was made on the left flank and the left kidney was visualized. The left kidney was then injected subcapsularly with 50 μl hydrogel containing bFGF or EGF. Control animals received hydrogel without GFs. Wounds were closed with a two-layer wound closure. 24- and 42 h after hydrogel injection, BrdU was injected (intra peritoneal) into mice (200 μl per animal (10 μg/ml)) for *in vivo* detection of proliferating cells. Animals were sacrificed 48 h after hydrogel injection. Kidney tissue was harvested and fixed in 10% formalin or frozen in OCT (Tissue-Tek, Sakura FineTek, Torrance, CA, USA). Blood was collected for separation into serum. Studies were conducted in accordance with the National Institute of Health Guide for the Care and Use of Laboratory Animals.

2.9. Histological analysis

Renal histology was performed on paraffin embedded formalin fixed biopsy sections (5 μm) stained with haematoxylin & eosin (H&E, Vector Laboratories, Burlingame, CA, USA). Luminal hyaline casts and tissue necrosis were counted in > 25 high-power fields (× 40) (non-overlapping), in a single-blinded fashion as described [35]. Proliferation of tubular epithelial cells was quantified using BrdU staining, performed as described previously [35]. Antigens were unmasked by boiling tissue sections in citrate buffer (0.01 mM) for 15 min. Sections were blocked with 5% bovine serum albumin in PBS and stained with monoclonal anti-BrdU antibody (1:25, Dako Cytomation, Dako, Carpinteria, CA, USA) for 60 min at RT. Anti-mouse horseradish peroxidase-conjugated antibody (Pierce, Rockford, IL, USA) was used as a secondary antibody (1:300, 60 min, RT). BrdU-positive cells were quantified by counting positive nuclei in 20 non-overlapping high-power fields (× 40) chosen randomly in the cortex of the kidney section (For the detailed statistic description see Supplemental material.).

3. Results and discussion

3.1. Design of starPEG-heparin hydrogel network

We chose to use a hydrogel as the material for our experimental system as it closely matches the properties of the natural ECM. It is vital that the mechanical characteristics (swelling, stiffness and mesh size) of the materials can be measured and preferably controlled, so they can be tailored to different clinical applications. This can be achieved by using starPEG-heparin gels, as the mechanical properties of starPEG-heparin gels can be manipulated by varying the degree of gel crosslinking [15] and [16]. The 14 kDa heparin used in this study has 24 carboxylic groups on average and can be cross-linked by carbodiimide with the four amino groups of end-functionalized starPEG (10 kDa). The creation of amide bonds between the amino groups of starPEG and the carboxylic groups of heparin leads to the formation of a highly hydrated binary polymer network, a hydrogel. The crosslinking degree in such material can be easily modulated by using different ratios of heparin and starPEG molecules which allows the creation of a series of hydrogels with a well-defined range of reproducible mechanical properties. An important advantage of this approach is that the total heparin concentration is independent of the crosslinking degree (which determines gel stiffness) in the fully hydrated, swollen gels (about 10 mg/ml). Heparin concentration dictates GF binding and release characteristics independently from the gels' mechanical properties [17]. Therefore, this approach can be applied to provide similar GF release rates for a wide variety of gel mechanical characteristics suitable for the creation of injectable gels. Assuming the injectable gel has to be relatively soft (low elastic modulus) to be delivered by a syringe, we focused on a hydrogel with a molar ratio of starPEG to heparin of 1.5.

3.2. Formation of starPEG-heparin gel particles

Our approach was based on a “top-down” strategy, in which we transferred a bulky hydrogel of known structure and properties into gel particles of μm-scale. The gel particles were created by mechanically breaking up the starPEG-heparin hydrogel network. To create injectable properties and narrow the dispersity of particle size, the gel was pushed through syringe needles with decreasing diameter. The aim was to produce injectable hydrogel particles which have similar microscopic properties (mesh-size and chemical structure), but differing material properties (viscosity) from the original hydrogel.

The hydrogel particles were able to form non-covalent aggregates that held the gel together as shown in Fig. 2A. Confocal microscopy was used to characterize the shape and size of the particles. During air

exposure the hydrogel loses water and consequently its shape. This process is dramatically accelerated in μm-scale particles, which makes it difficult to measure their swollen state. The best contrast for the hydrogel particles was observed on the interface of an aqueous solution (Fig. 2B). The needle's internal diameter of 0.26 mm (26G) was the limiting size in particle formation and therefore the particles were expected to be smaller than 260 μm. This was supported by the measurements of the images from DIC microscopy. Simple statistics of the particle size distribution revealed a large size dispersion, with the majority of the particle's average diameter being within 25–50 μm (Fig. 2C). After breaking up the gel to smaller particles, the material still kept its original biochemical properties, but the non-covalent nature of the particles' interaction provided the necessary viscoelastic properties. Originally, there was no intention to create particles with a narrow size distribution because in such a system particles have more free space to move around. This makes their friction and therefore viscous behavior low. On the other hand, in a hydrogel system with a wide size distribution, particles will pack more densely and therefore have higher elastic (Young's modulus) characteristics. Theoretically, the macroscopic characteristic of the hydrogel particles can be manipulated not only by the intrinsic stiffness of the hydrogel particles but also through “starching” or “tightening up” the particle size distribution.

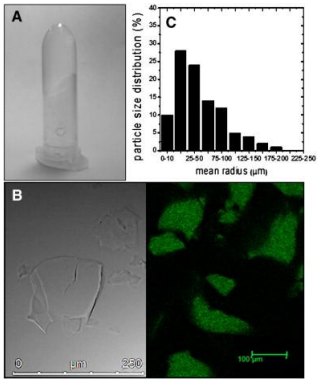

Fig. 2.

starPEG-heparin particles.

(A) Photograph of a vial with a starPEG-heparin hydrogel particle aggregate. (B) Differential interference contrast image of gel particles obtained by light and fluorescence microscopy. (C) The distribution of the average size of the gel particles.

3.3. Network structure and physical characteristics

Hydrogel material injected into a tissue can undergo mechanical stress during ambulation and should provide some resistance to the applied forces to maintain its mechanical and morphological characteristics. In other words, the gel should have significant elastic properties to prevent its migration from the injected area which is expected for viscous liquids. Oscillatory rheometry measurements were used to examine the viscous and elastic properties of the material as a response to cyclical shear forces. The storage modulus *G*′ describes the stiffness or elastic character of a material and the loss modulus *G*″ describes its viscous properties. For bulk hydrogel material, before it is broken into hydrogel particles, (Fig. 3A) the storage modulus *G*′ is an order of magnitude higher (14 kPa) than the loss modulus *G*′ (0.08 kPa). The values of *G*′ and *G*″ are constant at all frequencies, which suggests that the shear stress spreads evenly along the hydrogel network, a typical characteristic of highly elastic materials such as cross linked hydrogel networks [38].

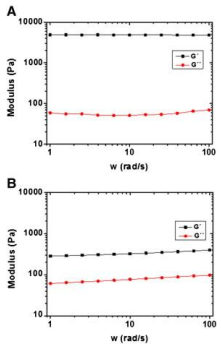

Fig. 3.

Oscillatory rheometry of the hydrogel. Oscillatory rheometry measurement of the covalently cross-linked (A) intact starPEG-heparin hydrogel and (B) starPEG-heparin hydrogel particles. Black symbols are storage moduli G' and red symbols are loss moduli G" in Pa.

Storage and loss moduli depend on hydrogel microstructure; when the gel is broken into particles, the stiffness of the particles itself should not change, but the stiffness of the gel-like aggregates (particle assemblies) should decrease. This is observed in Fig. 3B as the absolute value of *G*' drops when the viscosity slightly increases as the *G*" rises. Nevertheless, the *G*' value (300 Pa) of the particle mixture is still higher than *G*" (90 Pa) and their difference is almost constant at all frequencies. Such material can therefore be considered a gel network [39], [40] and [41]. The stiffness of the particle aggregates is approximately 300 Pa, which is similar to the softest hydrogel created by covalent crosslinking of heparin and starPEG [16].

The results of the rheometry measurements suggest that the hydrogel particles could also be considered as a prospective filler for medical or cosmetic use, where the gel properties could be refined for custom applications. The mechanical characteristics of the hydrogel particles determine the injection properties, an important factor for therapeutic use. The characteristics of the injectable hydrogel can be modulated by selecting the size and dispersity of particles, as well as the mechanical characteristics of its original starPEG-heparin hydrogel network. Therefore, the approach presented here provides enough triggers to attain the desired injectable characteristics, providing a number of options for its application as both an inert filler and a GF delivery system.

3.4. Growth factor release studies

The release properties of GFs from a starPEG-heparin hydrogel have been previously described by our group [17] and [18]. GF release depends on the surface area of the hydrogel. The hydrogel particles have an extensive surface area in comparison to the bulk hydrogel material and, therefore, the release kinetics were re-evaluated. Release of bFGF (Fig. 4A) was performed under previously described conditions [39] that recreate an *in vitro* situation close to the *in vivo* environment. Additionally, we show the release kinetics of EGF from a heparin containing hydrogel (Fig. 4B) that has not to our knowledge been previously reported.

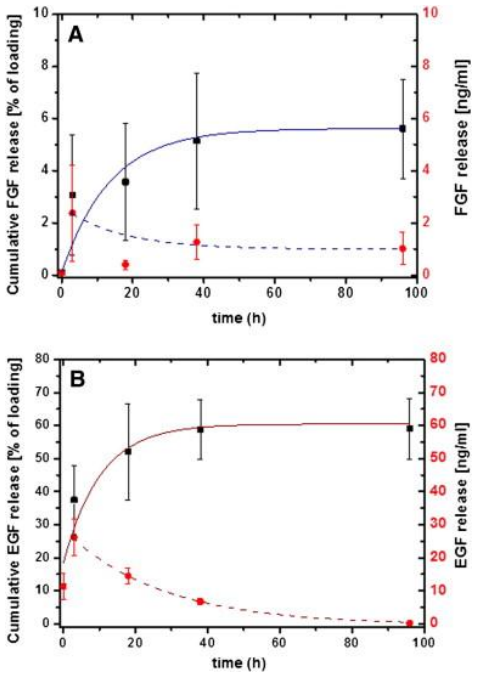

Fig. 4.

Release of growth factors. (A) Cumulative release of bFGF (black dots) and the measured concentration of the released bFGF at different time points (red dots). (B) Cumulative release of EGF (black dots) and the measured concentration of the released EGF at different time points (red dots).

Cumulative release of either bFGF or EGF was measured over four days with most of the sampling done during the first 48 h (corresponding to the duration of the *in vivo* experiment). The applied concentration of both GFs was the same (1 µg/ml), which is far below the concentration of heparin (1 µg/µl) in the hydrogel. Thus, a direct comparison of the kinetics of GF release, without heparin saturation, was possible. The initial wash of the samples with PBS (time point 0) revealed that bFGF had completely bound to heparin, as less than 0.2% of the loaded GF was unbound and "freely" present in the solution. In contrast, 11% of "free" EGF was found in the wash solution, indicating a clear difference in their heparin affinity. Within the first 3 h (the second time point) the release curves showed a typical burst for both of the GFs. The absolute values of the EGF release were order of magnitude higher (26 ng/ml) than for bFGF (2.4 ng/ml). The next 40 h showed release of the GFs with the total release of about 5 ng/ml of bFGF (~ 5% of the loaded GF) in contrast to almost 60 ng/ml of EGF (~ 60% of the loaded GF). The measurements at 96 h (the last time point) revealed the continuous released of bFGF with additional 1 ng/ml released from the gel while EGF release nearly stopped (less than 1 ng/ml is released). Hence, these release experiments illustrate the difference in the specific and non-specific binding of the GFs to heparin within the hydrogel particles. Even though the proposed delivery system is not suitable for long-term EGF release applications, short (40 h) experiments still seem to be reasonable.

3.5. Experimental AKI as the model for growth factor delivery

Experimental kidney injury models provide a convenient platform to test *in situ* regeneration strategies due to the kidneys' paired anatomy. Both kidneys can be damaged by experimentally induced disease and only one kidney is treated. The local effect on the treated kidney and the systemic effect on the untreated kidney can be compared. Experimental AKI induced by glycerol injection is a well-established model [42]. Intramuscular glycerol injection causes rhabdomyolysis, the dissolution of muscle fiber and the release of myoglobin from muscle cells. Binding of myoglobin to receptors in turn causes tubular injury. The characteristic histological damage includes acute necrosis of the distal tubes and the collecting ducts.

Tissue injury is visible on the structural and ultra-structural level, as it includes swelling of tubular cells and vacuolization of the cytoplasm, loss of brush border protein, as well as nuclear condensation [43]. Glycerol induced injury reaches a maximum between days 3 and 5 post injection, and is reversed within 15 days. To show that the GFs released from the hydrogel affected the surrounding tissue locally, only one kidney (Fig. 5A + B) was injected with GF-containing hydrogel. The working hypothesis was that the concentration of the released GF should be high enough to cause a local effect, but too low to cause a systemic effect. The kidney capsule is a natural barrier, which needs to be overcome for successful drug delivery. Insertion of implants under the kidney capsule is not a trivial procedure, which often involves tissue trauma and consequent inflammation issues. Injection, a minimally invasive technique, is clearly more attractive because of its simplicity (Fig. 5B) and the significant decrease in possible complications.

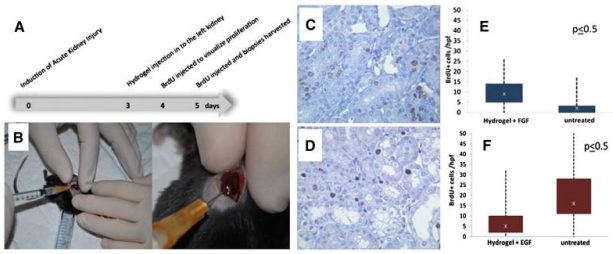

Fig. 5.

In vivo growth factor delivery in a model of AKI. (A) Acute kidney injury was induced by intramuscular glycerol injection (7.5 g/kg bodyweight) at day 0. At day 3 the animals received a subcapsular hydrogel injection into the left kidney. To detect cell proliferation, the animals were injected intraperitoneally with 2 mg BrdU on days 4 and 5. Tissue samples were collected on day 5. (B) The left kidney was injected with 50 μl hydrogel containing bFGF or EGF. The injection was made under the left kidney capsule and the right kidney remained untreated. (C and D) Proliferation of tubular cells. Representative images showing BrdU positive cells (brown) in (C) hydrogel + bFGF and in (D) the non-injected contralateral kidney. BrdU positive cells were counted in tissue sections of animals injected with (E) hydrogel + bFGF or (F) hydrogel + EGF into the left kidney. The right kidney remained untreated. BrdU positive cells are shown as BrdU positive cells per high power field (× 40).

3.6. Injection of hydrogel loaded with growth factors in animals with AKI

Visual examination of the injected kidneys revealed the stability of the injected gel during the *in vivo* experiments. Wound healing was normal, without visual signs of inflammation for both the control and the GF treated animals. The sham treated animals, injected with hydrogel that did not contain GFs, (n = 3) did not show significant differences in tubular proliferation between the left injected (0.25 ± 0.1) and the right non-injected (0.28 ± 0.14) kidney, suggesting that the hydrogel alone did not induce proliferation (Supplemental materials Table 1). A significantly different effect was observed when the hydrogel was loaded with GFs. We found that the bFGF + hydrogel injected left kidneys (n = 4) exhibited a significant higher number of BrdU positive cells (9.91 ± 4.31) per high power field (hpf) than the non-injected right kidneys (2.66 ± 1.55) (Fig. 5E). The working hypothesis was that the concentration of the released growth factor would be high enough to cause a local effect, but too low to cause a systemic effect after it was distributed in the body. The observed increased number of proliferating tubular cells in the non-injected right kidney, when compared with the cell proliferation in the control animals, is an indication of an unwanted systemic effect. Nevertheless, bFGF increased proliferation in the injected left kidney nearly three times more than on the untreated right kidney. This suggested that the factors released from the hydrogel triggered local effects. The proliferation data of tubular cells per mouse show that this difference between the treated and untreated kidneys was observed for all mice that received bFGF (Supplementary Table 1). We speculate that the systemic effect of the bFGF treatment could be decreased by a better hydrogel distribution under the kidney capsule or by simply lowering the bFGF concentration. Serum creatinine and BUN of treated animals did not differ from untreated control animals, *i.e.* showed no

significant improvement (data not shown). A long-term experiment is necessary to determine any effect of the proposed treatment using these markers.

Treatment of mice with EGF (n = 7) strongly increased the number of proliferating tubular cells compared with the control animals. However, the EGF-containing hydrogel showed an opposite local effect to the bFGF treatment. In particular, EGF treated left kidneys had a lower number of proliferating tubular cells (6.94 ± 2.35) than the non-injected right kidneys (19.35 ± 7.45) (Fig. 5F). The significant negative difference between the treated and untreated kidneys was observed for almost all mice treated with EGF (Supplemental material Table 1). The strong effect by EGF on the number of proliferating cells had clearly indicated the prospective of this GF for kidney injury treatments. It could be interpreted that the higher proliferation in the non-treated right kidney was due to EGF having a stronger systemic than local effect. However, the reduced proliferation in the EGF-containing hydrogel injected left kidney could be explained by a desensitization of the EGF receptor, as described before [44]. In other words, the local concentration of EGF in the left treated kidney was very high and induced not only the proliferation effect, but also the desensitization of the EGF receptor which correspondingly slowed the proliferation. It has been previously described by Yang et al. the injection of EGF (radiolabeled) in rats revealed after 4 h that the EGF mainly accumulated in the kidneys (12–20%) and to some extend in the liver (4–9%) [45]. Such accumulation of EGF in the kidney could explain the proliferative effect of EGF in the non-treated kidney. The amount of EGF distributed in the body and delivered into the right non-treated kidney could be closer to the optimum EGF concentration and induced a higher proliferation of tubular cells. This hypothesis is supported by the *in vitro* release experiments, where the low affinity of EGF to heparin results in a high (one order of magnitude greater than bFGF) release rate and, thus, a higher concentration in the injected area. Together, these results revealed the benefits of EGF for kidney regeneration, where the absolute value in cell proliferation (19.35 ± 7.45) for EGF treated mice was almost twice the absolute value (9.91 ± 4.31) observed for bFGF treated mice.

3.7. Analysis of growth factor release kinetics

The results of the *in vivo* experiment reveal possible benefits of EGF growth factor for kidney regeneration if an appropriate amount is delivered. In order to evaluate if a decrease of the loaded EGF concentration influence its release kinetics we compared a set of *in vitro* release experiments for the hydrogel with different amounts of EGF loaded amount of EGF (Fig. 6). The decrease of the EGF loaded concentration on 30% (0.7 μg/ml) has not revealed any significant difference in the release kinetics where about 50% is released within the first 40 h with about two third of this amount being released within the first 3 h of the experiment (Fig. 6A). Further 30% decrease of the EGF loaded concentration (0.4 μg/ml) revealed some differences in the release kinetics where about 33% of EGF is released within the first 40 h. The observed values of EGF release are still more than order of magnitude higher than the measured for the bFGF release (Fig. 6A). Moreover, the 60% decrease of EGF loaded amount still release in absolute amount in 3 times more of the GF compared to original bFGF concentration (Fig. 6B). Differently from the bFGF behavior, all of the loaded EGF concentration revealed the presence of unbound GF which is “freely” present in the solution at the start point. Together it suggests that simple decrease in the loaded concentration is a poor solution for EGF controlled release by proposed hydrogel system. The creation of EGF with a heparin tag could potentially overcome the observed behavior and act similarly to heparin binding GF such as bFGF.

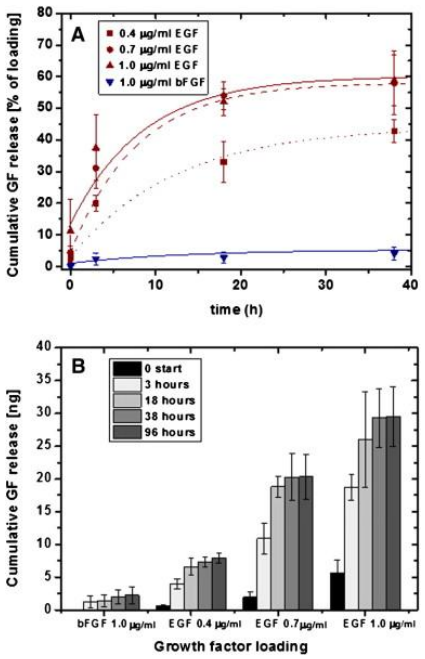

Fig. 6.

Comparison analysis of the release kinetics. (A) Cumulative release in percent from the loading amount of EGF of 0.4 mg/ml (red squares dot line), 0.7 µg/ml (red circles dash line), 1 µg/ml (red triangles solid line) and bFGF 1 µg/ml (blue triangles solid line). (B) Cumulative amount of the released GFs at different time points.

4. Conclusion

The present study aimed to expand the relevant properties of starPEG-heparin hydrogels by changing the gel morphology and developing mechanical properties suitable for injection. We intended to create hydrogel particles in order to apply them in *in vivo* experiments, in which the hydrogel would function as a local deposit for GFs capable of stimulating paracrine effects upon release. The produced starPEG-heparin hydrogel was tested as a local GF delivery system in an experimental model for AKI. To compare local and systemic effects, the hydrogels were injected in the left kidney of mice with AKI and tubular cell proliferation was compared between the injected and non-injected kidney. Kidneys injected with bFGF-containing hydrogel showed a significantly higher number of proliferating tubular epithelial cells after 48 h than the non-injected right kidneys. Additionally, this research has revealed the benefits of EGF for kidney regeneration where a significant effect in cell proliferation can be observed for 50 ng of the locally delivered GF in comparison to the 20 µg dose previously described for subcutaneous GF administration [34]. The simple lowering of the EGF loaded concentration has not dramatically changed the release kinetics. Nevertheless, the low affinity of EGF to heparin suggests that slowing the release kinetics by engineering EGF with a heparin tag could be beneficial in the kidney treatment.

The results from this work suggest that the proposed approach has great potential as a new system for the controlled release of GFs and can be a versatile instrument in regenerative therapies. A correlation was observed between *in vivo* and *in vitro* data, suggesting a similarity for the release mechanism in both experiments and the amount of the released GFs. While a suitable GF dose or a combination of GFs needs to be further evaluated, the novel starPEG-heparin hydrogel system offers valuable options to explore the impact of GF delivery properties on cell fate decisions, the stimulation of survival and proliferation [15] and [46]. Moreover, the implementation of controllable biodegradable properties [47], [48] and [49] in the

design of such hydrogel particles can further tune the release characteristics and expand their application in therapeutic approaches.

Acknowledgments

This work has been supported by the European Union through the 7FP projects (ANGIOSCAFF and KIDSTEM) and from the Deutsche Forschungsgemeinschaft (WE 2539-7/1, SFB 655 and FOR/EXC999). Financial support from Bundesministerium für Bildung, Forschung und Technologie (BMBF) through grant 01 GN 0946 is gratefully acknowledged. This study is also supported also by the National Research Council, Targeted Project Biotechnology and by Ministero Università e RicercaScientifica e Technologica (MURST) ex60%. Doctors Carvalhosa, Hauser and Tsurkan are Marie Curie Fellows within the Kidstem Project, funded by the European Community. Authors thank Dr. Kandice Levental for the critical discussion of the rheology data. Authors also thank Marcus Binner and Mirko Nowak for their help during the manuscript preparation.

References

[1] M.H. Little

Regrow or repair: potential regenerative therapies for the kidney

J. Am. Soc. Nephrol., 17 (2006), pp. 2390–2401

[2] K. Lee, E.A. Silva, D.J. Mooney

Growth factor delivery-based tissue engineering: general approaches and a review of recent developments

J. R. Soc. Interface, 8 (2011), pp. 153–170

[3] R. Vasita, D.S. Katti

Growth factor-delivery systems for tissue engineering: a materials perspective

Expert Rev. Med. Devices, 3 (2006), pp. 29–47

[4] K.N. Ekdahl, J.D. Lambris, H. Elwing, D. Ricklin, P.H. Nilsson, Y. Teramura, I.A. Nicholls, B. Nilsson

Innate immunity activation on biomaterial surfaces: a mechanistic model and coping strategies

Adv. Drug Deliv. Rev., 63 (2011), pp. 1042–1050

[5] I. Capila, R.J. Linhardt

Heparin–protein interactions

Angew. Chem. Int. Ed., 41 (2002), pp. 390–412

[6] D.S. Benoit, A.R. Durney, K.S. Anseth

The effect of heparin-functionalized PEG hydrogels on three-dimensional human mesenchymal stem cell osteogenic differentiation

Biomaterials, 28 (2007), pp. 66–77

[7] S.H. Kim, K.L. Kiick

Heparin-mimetic sulfated peptides with modulated affinities for heparin-binding peptides and growth factors

Peptides, 28 (2007), pp. 2125–2136

[8] T. Nie, A. Baldwin, N. Yamaguchi, K.L. Kiick

Production of heparin-functionalized hydrogels for the development of responsive and controlled growth factor delivery systems

J. Control. Release, 122 (2007), pp. 287–296

[9] I. Strehin, Z. Nahas, K. Arora, T. Nguyen, J. Elisseeff

A versatile pH sensitive chondroitin sulfate-PEG tissue adhesive and hydrogel

Biomaterials, 31 (2010), pp. 2788–2797

[10] G. Tae, Y.J. Kim, W.I. Choi, M. Kim, P.S. Stayton, A.S. Hoffman

Formation of a novel heparin-based hydrogel in the presence of heparin-binding biomolecules

Biomacromolecules, 8 (2007), pp. 1979–1986

[11] X. Zheng Shu, Y. Liu, F.S. Palumbo, Y. Luo, G.D. Prestwich

In situ crosslinkable hyaluronan hydrogels for tissue engineering

Biomaterials, 25 (2004), pp. 1339–1348

[12] M. Fujita, M. Ishihara, M. Simizu, K. Obara, T. Ishizuka, Y. Saito, H. Yura, Y. Morimoto, B. Takase, T. Matsui, M. Kikuchi, T. Maehara

Vascularization in vivo caused by the controlled release of fibroblast growth factor-2 from an injectable chitosan/non-anticoagulant heparin hydrogel

Biomaterials, 25 (2004), pp. 699–706

[13] M. Ishihara, K. Obara, T. Ishizuka, M. Fujita, M. Sato, K. Masuoka, Y. Saito, H. Yura, T. Matsui, H. Hattori, M. Kikuchi, A. Kurita

Controlled release of fibroblast growth factors and heparin from photocrosslinked chitosan hydrogels and subsequent effect on in vivo vascularization

J. Biomed. Mater. Res. A, 64 (2003), pp. 551–559

[14] D.B. Pike, S. Cai, K.R. Pomraning, M.A. Firpo, R.J. Fisher, X.Z. Shu, G.D. Prestwich, R.A. Peattie

Heparin-regulated release of growth factors in vitro and angiogenic response in vivo to implanted hyaluronan hydrogels containing VEGF and bFGF

Biomaterials, 27 (2006), pp. 5242–5251

[15] U. Freudenberg, A. Hermann, P.B. Welzel, K. Stirl, S.C. Schwarz, M. Grimmer, A. Zieris, W. Panyanuwat, S. Zschoche, D. Meinhold, A. Storch, C. Werner

A star-PEG-heparin hydrogel platform to aid cell replacement therapies for neurodegenerative diseases

Biomaterials, 30 (2009), pp. 5049–5060

[16] P.B. Welzel, S. Prokoph, A. Zieris, M. Grimmer, S. Zschoche, U. Freudenberg, C. Werner

Modulating biofunctional starPEG heparin hydrogels by varying size and ratio of the constituents

Polymers, 3 (2011), pp. 602–620

[17] A. Zieris, S. Prokoph, K.R. Levental, P.B. Welzel, M. Grimmer, U. Freudenberg, C. Werner

FGF-2 and VEGF functionalization of starPEG-heparin hydrogels to modulate biomolecular and physical cues of angiogenesis

Biomaterials, 31 (2010), pp. 7985–7994

[18] A. Zieris, S. Prokoph, P.B. Welzel, M. Grimmer, K.R. Levental, W. Panyanuwat, U. Freudenberg, C. Werner

Analytical approaches to uptake and release of hydrogel-associated FGF-2

J. Mater. Sci. Mater. Med., 21 (2010), pp. 915–923

[19] J. Cerda, N. Lameire, P. Eggers, N. Pannu, S. Uchino, H. Wang, A. Bagga, A. Levin

Epidemiology of acute kidney injury

Clin. J. Am. Soc. Nephrol., 3 (2008), pp. 881–886

[20] M. Tonelli, B. Manns, D. Feller-Kopman

Acute renal failure in the intensive care unit: a systematic review of the impact of dialytic modality on mortality and renal recovery

Am. J. Kidney Dis., 40 (2002), pp. 875–885

[21] K.D. Liu, P.R. Brakeman

Renal repair and recovery

Crit. Care Med., 36 (2008), pp. S187–S192

[22] L.C. Racusen

The morphologic basis of acute renal failure

Acute Renal Failure: A Comparison to Brenner and Rector's The Kidney (2001), pp. 1–12

[23] M.B. Herrera, B. Bussolati, S. Bruno, V. Fonsato, G.M. Romanazzi, G. Camussi

Mesenchymal stem cells contribute to the renal repair of acute tubular epithelial injury

Int. J. Mol. Med., 14 (2004), pp. 1035–1041

[24] M. Morigi, B. Imberti, C. Zoja, D. Corna, S. Tomasoni, M. Abbate, D. Rottoli, S. Angioletti, A. Benigni, N. Perico, M. Alison, G. Remuzzi

Mesenchymal stem cells are renotropic, helping to repair the kidney and improve function in acute renal failure

J. Am. Soc. Nephrol., 15 (2004), pp. 1794–1804

[25] B.D. Humphreys, J.V. Bonventre

The contribution of adult stem cells to renal repair

Nephrol. Ther., 3 (2007), pp. 3–10

[26] S. Bruno, C. Grange, M.C. Deregibus, R.A. Calogero, S. Saviozzi, F. Collino, L. Morando, A. Busca, M. Falda, B. Bussolati, C. Tetta, G. Camussi

Mesenchymal stem cell-derived microvesicles protect against acute tubular injury

J. Am. Soc. Nephrol., 20 (2009), pp. 1053–1067

[27] E.J. Sharples

Acute kidney injury: stimulation of repair

Curr. Opin. Crit. Care, 13 (2007), pp. 652–655

[28] S. Wang, R. Hirschberg

Role of growth factors in acute renal failure

Nephrol. Dial. Transplant., 12 (1997), pp. 1560–1563

[29] T. Takahashi, U. Huynh-Do, T.O. Daniel

Renal microvascular assembly and repair: power and promise of molecular definition

Kidney Int., 53 (1998), pp. 826–835

[30] F.P. Schena

Role of growth factors in acute renal failure

Kidney Int. Suppl., 66 (1998), pp. S11–S15

[31] E.J. Nouwen, W.A. Verstrepen, M.E. De Broe

Epidermal growth factor in acute renal failure

Ren. Fail., 16 (1994), pp. 49–60

[32] R.J. Anderson, C.J. Ray

Potential autocrine and paracrine mechanisms of recovery from mechanical injury of renal tubular epithelial cells

Am. J. Physiol., 274 (1998), pp. F463–F472

[33] G.T. Montelione, K. Wuthrich, A.W. Burgess, E.C. Nice, G. Wagner, K.D. Gibson, H.A. Scheraga

Solution structure of murine epidermal growth factor determined by NMR spectroscopy and refined by energy minimization with restraints

Biochemistry, 31 (1992), pp. 236–249

[34] H.D. Humes, D.A. Cieslinski, T.M. Coimbra, J.M. Messana, C. Galvao

Epidermal growth factor enhances renal tubule cell regeneration and repair and accelerates the recovery of renal function in postischemic acute renal failure

J. Clin. Invest., 84 (1989), pp. 1757–1761

[35] P.V. Hauser, R. De Fazio, S. Bruno, S. Sdei, C. Grange, B. Bussolati, C. Benedetto, G. Camussi

Stem cells derived from human amniotic fluid contribute to acute kidney injury recovery

Am. J. Pathol., 177 (2010), pp. 2011–2021

[36] M.B. Herrera, B. Bussolati, S. Bruno, L. Morando, G. Mauriello-Romanazzi, F. Sanavio, I. Stamenkovic, L. Biancone, G. Camussi

Exogenous mesenchymal stem cells localize to the kidney by means of CD44 following acute tubular injury

Kidney Int., 72 (2007), pp. 430–441

[37] A. Karihaloo, C. Nickel, L.G. Cantley

Signals which build a tubule

Nephron Exp. Nephrol., 100 (2005), pp. e40–e45

[38] M.A. Meyers, K.K. Chawla

Mechanical Behavior of Materials

(Second edition)Cambridge University Press, Cambridge (2009)

[39] I. Levental, P.C. Georges, P.A. Janmey

Soft biological materials and their impact on cell function

Soft Matter, 3 (2007), pp. 299–306

[40] A. Omari, R. Tabary, D. Rousseau, F.L. Calderon, J. Monteil, G. Chauveteau

Soft water-soluble microgel dispersions: structure and rheology

J. Colloid Interface Sci., 302 (2006), pp. 537–546

[41] P.K. Vemula, E. Boilard, A. Syed, N.R. Campbell, M. Muluneh, D.A. Weitz, D.M. Lee, J.M. Karp

On-demand drug delivery from self-assembled nanofibrous gels: a new approach for treatment of proteolytic disease

J. Biomed. Mater. Res. A, 97 (2011), pp. 103–110

[42] G.A. Tanner

Experimental models of acute tubular necrosis

S.R.A.a.J.A. Thornhill (Ed.), CRC Handbook of Animal Models of Renal Failure, CRC Press, Boca Raton, FL (1985), pp. 109–144

[43] X. Bosch, E. Poch, J.M. Grau

Rhabdomyolysis and acute kidney injury

N. Engl. J. Med., 361 (2009), pp. 62–72

[44] J.L. Countaway, A.C. Nairn, R.J. Davis

Mechanism of desensitization of the epidermal growth factor receptor protein-tyrosine kinase

J. Biol. Chem., 267 (1992), pp. 1129–1140

[45] W. Yang, R.F. Barth, R. Leveille, M. Ciesielski, R.A. Fenstermaker, J. Capala

Evaluation of systemically administered radiolabeled epidermal growth factor as a brain tumor targeting agent

J. Neurooncol., 55 (2001), pp. 19–28

[46] A. Zieris, K. Chwalek, S. Prokoph, K.R. Levental, P.B. Welzel, U. Freudenberg, C. Werner

Dual independent delivery of pro-angiogenic growth factors from starPEG-heparin hydrogels

J. Control. Release, 156 (2011), pp. 28–36

[47] K. Chwalek, K.R. Levental, M.V. Tsurkan, A. Zieris, U. Freudenberg, C. Werner

Two-tier hydrogel degradation to boost endothelial cell morphogenesis

Biomaterials, 32 (2011), pp. 9649–9657

[48] M.V. Tsurkan, K. Chwalek, K.R. Levental, U. Freudenberg, C. Werner

Modular StarPEG-Heparin Gels with Bifunctional Peptide Linkers

Macromol. Rapid Commun., 31 (2010), pp. 1529–1533

[49] M.V. Tsurkan, K.R. Levental, U. Freudenberg, C. Werner

Enzymatically degradable heparin-polyethylene glycol gels with controlled mechanical properties

Chem. Commun. (Camb.), 46 (2010), pp. 1141–1143